American Mineralogist, Volume 62, pages 475–490, 1977

Titanium-containing silicate garnets. I. The distribution of Al, Fe^{3+}, and Ti^{4+} between octahedral and tetrahedral sites

FRANK E. HUGGINS, DAVID VIRGO AND H. GERHARD HUCKENHOLZ[1]

Geophysical Laboratory, Carnegie Institution of Washington
Washington, D. C. 20008

Abstract

The distribution of ferric iron between octahedral and tetrahedral sites in synthetic titanium garnets of compositions between $Ca_3Fe_2Ti_{1.42}Si_{1.58}O_{12}$ (50:50 by weight $Ca_3Fe_2Si_3O_{12}$:$Ca_3Fe_2Ti_3O_{12}$), and both $Ca_3Al_2Si_3O_{12}$ and $Ca_3Fe_2Si_3O_{12}$ have been measured by ^{57}Fe Mössbauer spectroscopy. By using an ideal cation-exchange model in conjunction with the ferric distribution data, the distribution of aluminum and titanium in the garnet structure can also be obtained. The distribution of Al, Fe^{3+}, and Ti^{4+} between the sites approaches equilibrium only at temperatures in excess of 1200°C over a period of weeks; it appears, however, that the relative preference for the tetrahedral site must be in the order Al ≥ Fe > Ti. This order of preference is inconsistent with crystal-chemical guidelines based only on ionic size and charge, and an additional factor, electronegativity, is necessary to rationalize the inferred site preferences.

At temperatures of 1050°C and below, the measured ferric distribution in these garnets synthesized from glasses is inconsistent with an equilibrium distribution, because the same distribution is observed at different temperatures for a given composition. It is therefore inferred that such temperature-independent distributions result from the extremely slow kinetics for the cation exchange, that effectively eliminates observing any change in the distribution during the synthesis of the garnets. Such frozen-in, initial distributions appear to reflect the crystallization path. In particular, the presence of $CaSiO_3$ or $CaTiO_3$ as intermediate and metastable products in the crystallization process is correlated with the observed cation distribution in garnets synthesized below 1050°C. The ferric distributions in titanium garnets formed from gels or in natural garnets associated with serpentized peridotites differ significantly from those in garnets synthesized from glasses, and most probably reflect quite different crystallization reactions.

Introduction

Natural titanium-rich garnets, usually known as melanites or schorlomites, differ markedly from other natural garnets. For instance, their main petrologic occurrence is in undersaturated alkaline igeneous rocks, unlike most other garnets, which are found predominantly in metamorphic environments. In addition, the chemistry of titanium-rich garnets is also significantly more complicated, because silicon does not completely fill the tetrahedral sites and there is usually an excess of divalent cations (X) and a deficiency of trivalent cations (Y) indicated by chemical analyses when compared with the usual garnet formula, $X_3Y_2Si_3O_{12}$. For these reasons, the crystal chemistry of natural titanium garnets poses a number of interesting problems not encountered with other silicate garnets. In particular, the relative site preferences of Al, Fe^{3+}, and Ti between the octahedral sites and those tetrahedral sites not occupied by silicon, and the oxidation states of iron and titanium in the garnets are two problems that have been extensively discussed in the literature. Almost without exception, such discussions have been based on studies of a suite of natural samples of different compositions and parageneses lacking sufficient control of the several variables to give definitive answers.

The present study of titanium garnets differs from previous investigations in that an attempt has been made to establish an experimental framework in

[1] Permanent address: Mineralogisch-Petrographisches Institut der Universität, München, West Germany.

which the crystal chemistry of titanium garnets may be interpreted. In this paper, the relative site preferences of Al, Fe^{3+}, and Ti^{4+} for the octahedral or tetrahedral sites in the garnet structure are discussed; in subsequent papers, the phase equilibria, the intrinsic oxygen fugacities, and the oxidation states of titanium and iron in natural melanites and schorlomites will be discussed.

The distribution of Al, Fe, and Ti in the garnet structure can, in principle, be resolved by combined X-ray and neutron diffraction studies. Such studies of natural garnets have not been reported, however, and attempts to establish the site distribution of these cations have been based on results of other techniques or crystal-chemical principles. Unfortunately, vibrational spectra of titanium garnets and studies of correlations between the elements in garnets do not yield an unambiguous assignment of the cations to the sites.

Vibrational spectra of titanium garnets were originally interpreted (Tarte, 1959) as indicating the replacement of Si in the tetrahedral sites by Ti. Subsequently, however, Tarte (1965) and Howie and Woolley (1968), although maintaining this interpretation, expressed reservations about its uniqueness. Recently, Dowty and Mark (1968), Moore and White (1971), and Dowty (1971) suggested that the vibrational spectra could actually be better interpreted as Al^{3+} or Fe^{3+} replacing Si in the tetrahedral sites.

Attempts to ascertain the location of Ti^{4+} in the garnet structure have also been based on elemental correlations from chemical analyses of natural garnets and, in particular, from the relationships between Si, Fe^{3+}, Al^{3+}, and Ti^{4+} in zoned crystals. In such analyses, an inverse relationship noted between Si and Ti^{4+} (Kunitz, 1936; Howie and Woolley, 1968) was offered as evidence that Ti^{4+} principally replaces Si in the structure. Contrasting inverse elemental correlations, however, such as that between Ti^{4+} and Fe^{3+} (Lehijärvi, 1967; Isaacs, 1968), indicate that this explanation is not sufficient for all cases. In any case, the ratio of Ti to the number of tetrahedrally coordinated sites not occupied by Si is uniformly in excess of 1:1, demonstrating that Si is not the only element being replaced by Ti.

Mössbauer studies of natural garnets (Dowty, 1971; Burns, 1972) showed that ferric iron can enter the tetrahedral sites, but did not resolve the question of whether Ti^{4+} or Al filled the remaining tetrahedral sites. Burns and Burns (1971) reported Mössbauer data from some titanian garnets of different parageneses, most of which indicated the presence of both octahedral and minor tetrahedral ferric iron. However, garnets from serpentinized peridotites exhibit only octahedral ferric iron in their Mössbauer spectra (Burns and Burns, 1971), indicating that ferric iron was completely absent from the tetrahedral sites. In contrast, Burns (1972) reported the Mössbauer spectrum of a garnet of composition $Ca_3[Fe^{3+}Ti](Fe^{3+}Si_2)O_{12}$ that had been synthesized by heating coprecipitated gels for 20 hours at 1050°C (Ito and Frondel, 1967), which indicated that ferric iron completely filled the tetrahedral sites not occupied by silicon. Hence, it might be inferred that the cation distribution observed in titanian garnets can be determined by the conditions of synthesis.

Synthesis and phase-equilibrium studies of titanium iron silicate garnets (Ito and Frondel, 1967; Huckenholz, 1969) are inconclusive because compositions more titanium-rich than $Ca_3Fe_2Ti_{1.5}Si_{1.5}O_{12}$ are not stable at 1 atm (Huckenholz, 1969), and so either Fe^{3+} or Ti^{4+} or both could make up the silicon deficiency. The replacement of Fe^{3+} by Al^{3+} in such garnets further reduces the maximum amount of titanium that can be substituted in the garnet (Hölzl, 1975), and again such studies are not informative for assessing site preferences. If Zr^{4+} fills the octahedral site in the garnet structure, Ti^{4+}, can enter the tetrahedral site, as evidenced by the formation of $Ca_3Zr_2(TiFe_2)O_{12}$ (Ito and Frondel, 1967). Studies of other titanium-substituted, nonsilicate garnet systems (Espinosa, 1964; Geller *et al.*, 1965), have indicated, on the basis of measurements of the magnetic properties of the garnets, that the substitution of Ti^{4+} in yttrium iron garnet may be an order-disorder phenomenon, with ferric iron favoring the tetrahedral site over titanium. The possibility that this kind of phenomenon might also be found in titanium-containing silicate garnets and hence that natural garnets may be used as geothermometers has not been investigated.

In this paper, results of a ^{57}Fe Mössbauer study of synthetic garnet solid-solutions between the composition $Ca_3Fe_2Ti_{1.42}Si_{1.58}O_{12}$ (hereafter referred to as TIAN) and either $Ca_3Al_2Si_3O_{12}$ (GR) or $Ca_3Fe_2Si_3O_{12}$ (AN) are presented. The composition $Ca_3Fe_2Ti_{1.42}Si_{1.58}O_{12}$ was used because it is close to the maximum extent of solid solution between $Ca_3Fe_2Si_3O_{12}$ and the hypothetical garnet $Ca_3Fe_2Ti_3O_{12}$, and corresponds to a 50:50 mixture by weight of $Ca_3Fe_2Si_3O_{12}$ and $Ca_3Fe_2Ti_3O_{12}$. The Mössbauer effect provides information directly concerning the site distribution of iron; however, the site distributions of Ti and Al

Table 1. Compositions of synthetic garnets investigated in this study

AN–TIAN join					GR–TIAN join					
	(x)*	Si pfu†	Ti pfu	Fe pfu		(x)	Si pfu	Ti pfu	Fe pfu	Al pfu
Andradite	0.000	3.000	0.000	2.000	Grossular	0.000	3.000	0.000	0.000	2.000
	0.387	2.451	0.549	2.000		0.174	2.754	0.246	0.347	1.653
	0.487	2.311	0.689	2.000		0.265	2.625	0.375	0.529	1.471
	0.587	2.168	0.832	2.000		0.359	2.492	0.508	0.718	1.282
	0.706	2.000	1.000	2.000		0.456	2.354	0.646	0.913	1.087
	0.854	1.791	1.209	2.000		0.558	2.211	0.789	1.115	0.885
Titan	1.000	1.584	1.416	2.000		0.662	2.062	0.938	1.324	0.676
						0.771	1.909	1.091	1.541	0.459
						0.883	1.749	1.251	1.766	0.234
					Titan	1.000	1.584	1.416	2.000	0.000

*Mole fraction TIAN.
†Per formula unit (12 oxygens).

can be inferred by difference or by using a thermodynamic model for the cation-exchange processes. By measuring samples prepared at different temperatures, the temperature dependence of the site distribution can be evaluated, from which the potential of natural titanium garnets as geothermometers may be assessed. In addition, the crystallochemical factors such as ionic charge, ionic radius, and electronegativity, which may determine the relative distribution of cations between the octahedral and tetrahedral sites in the garnet structure, are reexamined.

Experimental

Synthesis and composition of garnets

The samples used in this study were, for the most part, originally prepared in studies of the phase equilibria across the joins between AN and the hypothetical garnet $Ca_3Fe_2Ti_3O_{12}$ (Huckenholz, 1969), and between GR and TIAN (Hölzl, 1975; Hölzl and Huckenholz, in preparation). In both studies, the garnet starting materials were glasses prepared by rapidly quenching mixtures of the required amounts of oxides melted at temperatures between 1400° and 1500°C over a period of hours in air. Single-phase garnets were crystallized from the glasses at subsolidus temperatures using one of three methods. For the AN–TIAN compositions and for compositions along the GR–TIAN join stable at 1050°C, 5 g quantities of material were prepared in air and held at 1050°C for several weeks using platinum crucibles. To ensure homogeneous products, the glasses were ground intermittently. For compositions on the GR–TIAN join that are not stable at 1050°C (Hölzl, 1975), 500 mg quantities of garnets were crystallized at 800°C in standard hydrothermal equipment under 1 kbar of water pressure. The glasses were placed in gold capsules along with sufficient PtO_2 and H_2O to ensure a wet, oxidizing environment. The crystallization times in these runs were between 2 and 4 weeks. Finally, all other crystallization and heating experiments were made on ~50 mg quantities of glass or garnet crystals held in Pt envelopes, using quenching furnaces. The durations of the experiments are given in Tables 2, 3, and 6. More detailed experimental descriptions, including phase characterizations, are given by Huckenholz (1969), Hölzl (1975), and Hölzl and Huckenholz (in preparation).

The compositions of the samples investigated are listed in Table 1. Compositions across the GR–TIAN join can be represented by the general formula

$$Ca_3Al_{2-2x}Fe_{2x}Ti_{1.42x}Si_{3-1.42x}O_{12} \quad 0 \leq x \leq 1$$

and those across the AN–TIAN join by

$$Ca_3Fe_2Ti_ySi_{3-y}O_{12} \quad 0 \leq y \leq 1.42$$

By making the substitution $1.42x = y$ in the latter formula, the two joins can be expressed in terms of the same compositional parameter, x.

Properties of these garnets, such as refractive indices, density, and cell parameters, are described elsewhere (Huckenholz, 1969; Virgo and Huckenholz, 1974; Hölzl, 1975; Hölzl and Huckenholz, in preparation). The extent of stable garnet formation in the compositional field AN–GR–$Ca_3Al_2Ti_3O_{12}$–$Ca_3Fe_2Ti_3O_{12}$, based on the studies of Huckenholz (1969) and Hölzl (1975), is shown in Figure 1. The compositions along the two joins discussed in this paper approach the limit of stable garnet formation in this system.

Table 2. Mössbauer data for the AN–TIAN join at 1050°C

(x)	T/t* (°C/days)	Peak line widths A_{IV}**	A_{VI}	A_C***	Area ratios Q†	R	Cation site occupancies Fe_{VI}	Fe_{IV},Ti_{VI}††	Ti_{IV}	K_2
0.000	1050/155	...	0.27	0.28	1.00	1.00	2.00	0.00	0.00	...
0.387	1050/58	0.35	0.32	0.35	1.03	0.75	1.50	0.50	0.05	0.30
0.487	1050/105	0.31	0.33	0.34	1.02	0.72	1.44	0.56	0.13	0.60
0.587	1050/58	0.31	0.34	0.34	1.02	0.67	1.34	0.66	0.18	0.55
0.706	1050/88	0.31	0.34	0.35	1.02	0.63	1.26	0.74	0.26	0.60
0.854	1050/68	0.33	0.34	0.35	1.01	0.51	1.02	0.98	0.23	0.24
1.000	1050/30	0.32	0.34	0.36	0.99	0.41	0.82	1.18	0.24	0.14

*Temperature in °C and time in days of experimental conditions for crystallization from glass.
**Roman numeral subscript refers to coordination number of site.
***Subscript C refers to composite peak at high velocity.
†Area(A_{IV} + A_{VI})/area(A_C).
††In this join Fe_{IV} and Ti_{VI} occupancies must be equal.

Mössbauer experimentation

From ^{57}Fe Mössbauer experiments, the oxidation state and location of iron cations within a crystal structure can often be identified, and values for the ferrous–ferric ratio and the ratio of iron between two or more sites can be estimated if more than one type of iron cation is present.

In this study, Mössbauer experiments were performed in transmission geometry using ^{57}Co in a palladium matrix as the source of γ rays. The energy spectrum was provided by the Doppler effect resulting from the source moving at a constant acceleration with respect to the stationary sample absorber. The source velocity varied by ±4.2 mm/sec. Two mirror-image spectra of each sample were recorded simultaneously in a 1024 multichannel analyzer, *i.e.* 512 channels per spectrum. The velocity calibration and zero-velocity point of the spectra were achieved by periodically measuring reference spectra of iron metal foil.

The sample absorbers were prepared from mixtures of finely powdered garnets and 100–125 mg of Lucite (Fisher Scientific Company, Fairlawn, N. J.), which were hot-pressed at 150°C into 1.25 cm diameter disks of about 0.1 cm thickness. Enough garnet was added to the Lucite so that the areal density of iron was between 3 and 5 mg/cm^2. This concentration usually resulted in an absorption effect for the largest peak of 6 to 10 percent (Fig. 2).

Data were usually accumulated until at least 250,000 counts/channel were obtained. The spectral data were then analyzed by means of a least-squares fitting program on a Univac 1108 computer. The program fits a specified number of Lorentzian-shaped peaks to the data by an iterative procedure until a test for convergence is satisfied. A typical fitted spectrum (one of the two mirror spectra) of a titanium garnet is

Table 3. Mössbauer data for the GR–TIAN join at 800° and 1050°C*

(x)	T/t (°C/days)	Peak line widths A_{IV}	A_{VI}	A_C	Area ratios Q	R	Site occupancies Fe_{IV}	Fe_{VI}	Error (pfu)
0.174	800/17	0.48	0.36	0.39	0.98	0.86	0.049	0.279	±0.005
0.265	800/18	0.43	0.34	0.37	0.99	0.82	0.095	0.435	±0.008
0.359	800/8	0.40	0.34	0.38	0.99	0.77	0.165	0.553	±0.011
0.457	800/20	0.39	0.34	0.36	1.01	0.74	0.238	0.676	±0.014
0.558	800/14	0.37	0.34	0.35	1.01	0.70	0.335	0.781	±0.017
0.558	1050/75	0.34	0.34	0.37	1.00	0.70	0.335	0.781	±0.017
0.662	1050/120	0.35	0.35	0.36	1.02	0.63	0.490	0.834	±0.020
0.771	1050/120	0.35	0.36	0.37	1.02	0.55	0.694	0.848	±0.023
0.883	1050/75	0.33	0.35	0.36	0.99	0.48	0.918	0.848	±0.026
1.000	1050/30	See Table 2.							

*Symbols as defined in Table 2.

Table 4. Ordering schemes considered for garnets across the GR–TIAN join

Ordering scheme*	Equation for $\underline{R}$†		Equation for Fig. 4
Al > > Fe > > Ti	$\underline{R} = 1.00$	$(0.0 \leq \underline{x} \leq 0.5855)$	(1)
	$\underline{R} = (2 - 1.416\underline{x})/2\underline{x}$	$(0.5855 \leq \underline{x} \leq 1.0)$	
Al > > Fe = Ti	$\underline{R} = 1.00$	$(0.0 \leq \underline{x} \leq 0.5855)$	(2)
	$\underline{R} = 0.5855/\underline{x}$	$(0.5855 \leq \underline{x} \leq 1.0)$	
Al > > Ti > > Fe	$\underline{R} = 1.00$	$(0.0 \leq \underline{x} \leq 1.0)$	(3)
Al = Ti > > Fe	(3) above		
Fe > > Al > > Ti	$\underline{R} = 0.292$		(4)
Fe = Al > > Ti	$\underline{R} = 1 - 0.708\underline{x}$		(5)
Fe > > Ti > > Al	(4) above		
Fe > > Ti = Al	(4) above		
Ti > > Al > > Fe	(3) above		
Ti > > Al = Fe	(3) above		
Ti > > Fe > > Al	(3) above		
Ti = Fe > > Al	$\underline{R} = 0.5855$		(6)
Al = Fe = Ti	$\underline{R} = 2/(2 + 1.416\underline{x})$		(7)

*In terms of preference for tetrahedral sites, $\underline{x} > > \underline{y}$ means completely ordered: all $\underline{x}$ in tetrahedral site before any $\underline{y}$; $\underline{x} = \underline{y}$ means completely disordered: $\underline{x}$ and $\underline{y}$ in tetrahedral sites in accord with bulk ratio.
†See equation 1 in text.

shown in Figure 2. Three peaks are apparent visually—although four peaks actually contribute to the spectral profile. The spectrum consists of two components, an octahedral ferric absorption and a tetrahedral ferric absorption, each contributing two peaks to the spectrum. The low-velocity peaks of the two components are well separated, but the high-velocity peaks overlap considerably, resulting in an apparent three-peak spectrum. The areas of the two peaks of each component should be equal; hence, the area of the composite peak at highest velocity should equal the sum of the areas of the tetrahedral peak at lowest velocity and the octahedral peak at intermediate velocity.

In this study, all spectra were fitted to three peaks of Lorentzian line-shape. As discussed previously (Weber *et al.*, 1975), this fitting procedure requires no constraints on any of the peak parameters and does not provide area ratios significantly different from those obtained with a constrained, four-peak fit. As also discussed previously, the quality of the data, and the least-squares fitting procedure were evaluated using the statistical parameters developed by Ruby (1973) and Dollase (1975). The following criteria were adopted as indicating acceptable data and fit. First, the error in MISFIT (Ruby, 1973), which is a measure of the quality of the data, had to be less than 0.05 percent. Secondly, the results from fitting the two mirror-image spectra obtained in each experiment had to give closely similar parameters. Thirdly, the sum of the areas of the two resolved low-velocity peaks had to be within ±3 percent of the area of the composite, high-velocity peak. If the data and fit met these requirements, the procedures outlined by Dollase (1975) were used to estimate errors in the various parameters.

For site distribution data, it is particularly important to assess the error in the area ratio, R, defined as follows:

$$R = 2(\text{area } A_{VI})/\text{area } (A_{IV} + A_{VI} + A_C) = Fe_{VI}/(Fe_{IV} + Fe_{VI}) \quad (1)$$

where A_{IV}, A_{VI}, and A_C, respectively, are the resolved octahedral, tetrahedral, and composite Mössbauer peaks (Fig. 2), and where Fe_{VI} and Fe_{IV}, respectively, are the octahedral and tetrahedral site occupancies of ferric iron. By equating directly peak areas and site occupancies, it is assumed that the recoil-free fractions for ferric iron in the two sites are equal and that no thick absorber corrections are necessary. Based on

Table 5. Values for the distribution coefficients K_1 and K_2 for the GR–TIAN join

T, °C	$\underline{K}_1$	$\underline{K}_2$	Order of tetrahedral site preference
1050	2.20 ± 0.20	0.15 ± 0.05	Al > Fe > Ti
800	0.70 ± 0.10	1.15 ± 0.10	Ti > Fe > Al

Table 6. Supplementary experiments*

(x)	T/t (°C/days)	Peak line widths			Area ratios		Site occupancies				
		A_{IV}	A_{VI}	A_C	Q	R					
(a) GR-TIAN join at 800°C							Fe_{IV}	Fe_{VI}	Error		
0.662	800/14	0.35	0.33	0.36	1.01	0.62	0.503	0.821	±0.020		
0.771	800/14	0.35	0.35	0.36	1.02	0.56	0.678	0.864	±0.023		
0.883	800/12†	0.33	0.35	0.36	1.00	0.48	0.918	0.848	±0.026		
(b) AN-TIAN join above 1200°C							Fe_{VI}	Fe_{IV},Ti_{VI}	Ti_{IV}	K_2	
0.387	1225/7	0.34	0.34	0.36	0.99	0.75	1.50	0.50	0.05	0.30	
0.487	1220/8	0.33	0.35	0.36	1.02	0.70	1.40	0.60	0.09	0.35	
0.587	1220/7	0.32	0.36	0.37	1.02	0.66	1.32	0.68	0.15	0.43	
0.706	1275/3	0.32	0.36	0.37	1.02	0.59	1.18	0.82	0.18	0.32	
0.854	1260/7	0.33	0.37	0.37	1.02	0.52	1.04	0.96	0.25	0.28	
1.000	1245/5	0.33	0.37	0.37	1.01	0.46	0.92	1.08	0.34	0.27	
(c) GR-TIAN join above 1200°C							Fe_{IV}	Fe_{VI}	Error		
0.771	1220/10†	0.34	0.38	0.37	1.01	0.56	0.678	0.864	±0.023		
0.883	1230/40†	0.33	0.36	0.37	1.00	0.51	0.865	0.901	±0.026		
1.000	1245/5	See Table 6(b).									

*Symbols as defined in Table 2.
†Heating experiments on garnets crystallized at 1050°C.

Dollase's scheme, the error in the area of peak A_{IV} would exceed ±10 percent when the tetrahedral occupancy of ferric iron was only about 10 percent of the total iron; however, the error in R was always between 1 and 2 percent regardless of composition. Hence, the errors in the site occupancies of ferric iron in this study are estimated to be ±0.03 cation per formula unit for the AN–TIAN series. Errors in Fe^{3+} site occupancies for compositions across the GR–TIAN join are less than ±0.03 cation per formula unit because of the smaller amounts of total iron.

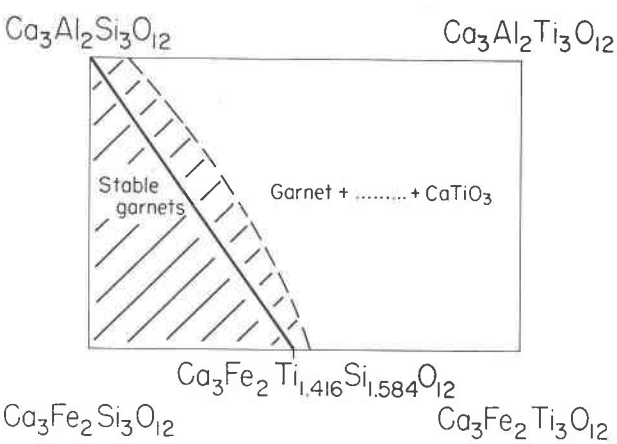

Fig. 1. Diagram locating the joins from along which compositions were used in this study. The maximum extent of stable garnet formation in the system $Ca_3Fe_2Si_3O_{12}$–$Ca_3Al_2Si_3O_{12}$–$Ca_3Fe_2Ti_3O_{12}$–$Ca_3Al_2Ti_3O_{12}$ is also shown.

No ferrous iron was detected in the Mössbauer spectra of any of the garnets, although 10–15 percent of the iron was in the ferrous state in the glasses. Owing to the oxidizing nature of the conditions under which the garnets were synthesized, it is assumed that Ti^{3+} is also absent.

Results

AN–TIAN join at 1050°C

The Mössbauer data and derived ferric site occupancies for samples along the AN–TIAN join are listed in Table 2. With increasing titanium content, the octahedral iron content decreases as shown graphically in Figure 3. Also shown in Figure 3 are calculated curves for the theoretical random distribution and for the ordered distributions corresponding to all titanium in either tetrahedral or octahedral coordination. By plotting between the random curve and the curve for the distribution that corresponds to all titanium in the octahedral sites, the data indicate that titanium enters the octahedral site in preference to ferric iron. It should be noted that the data show a

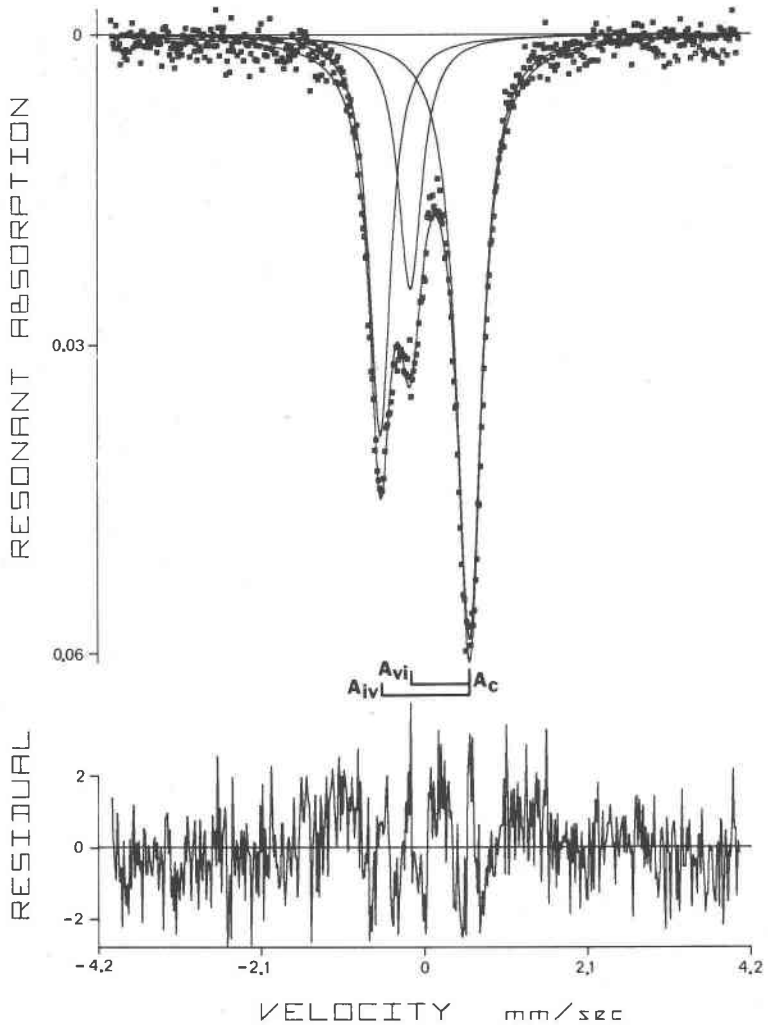

Fig. 2. Mössbauer spectrum of TIAN (x = 1.0). The data are fitted to three peaks: A_{VI}, tetrahedral component at low velocity; A_{VI}, octahedral component at low velocity; and A_C, a composite peak, resulting from the superposition of the octahedral and tetrahedral components at high velocity.

break in the trend between x = 0.7 and 0.85, which is also reflected in the values of K_2, the distribution coefficient, defined as follows:

$$K_2 = [Fe_{VI}][Ti_{IV}]/[Fe_{IV}][Ti_{VI}] \quad (2)$$

Values of K_2 (Table 2) suggest that either the distribution is not at equilibrium or cation exchange of Fe^{3+} and Ti^{4+} between the distinct sites does not conform to an ideal distribution model.

GR–TIAN join at 1050° and 800°C

The Mössbauer results for the GR–TIAN join are listed in Table 3. The data show a trend (Fig. 4) with increasing titanium content that is very similar to that of the AN–TIAN join. Also shown in Figure 4 are calculated curves for the extreme order or disorder schemes listed in Table 4. These curves show the calculated value for R at a given composition for a particular ordering scheme. Figure 4 shows that the experimental data do not match any of these schemes, although the data for low-titanium samples ($x \leq 0.6$) do plot close to the random model (Al = Fe = Ti). It is therefore inferred that the distribution is an order-disorder phenomenon.

Although Mössbauer experiments only provide data relating to the site distribution of ferric iron, by utilizing the compositional constraints on the join it is possible to evaluate the data in terms of an ideal cation-exchange model involving the distribution of and Ti^{4+}, Al^{3+}, and Fe^{3+} between the distinct sites. A

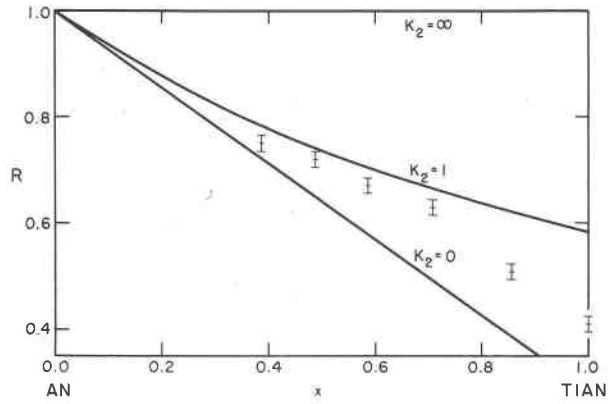

Fig. 3. Plot of the ferric distribution parameter, R, as a function of the compositional parameter, x, for samples along the AN–TIAN join synthesized at 1050°C. Also shown are curves corresponding to a random distribution of Fe^{3+} and Ti^{4+} ($K_2 = 1$) and to the ordered distributions where Ti enters the tetrahedral site ($K_2 = \infty$) or the octahedral site ($K_2 = 0$).

somewhat related approach was taken by Navrotsky (1975) in evaluating the site distributions, based only on Fe^{2+} Mössbauer data, of Fe^{2+}, Ti^{3+}, and Ti^{4+} in pseudobrookites between $FeTi_2O_5$ and Ti_3O_5.

In the synthetic GR–TIAN join, the following compositional constraints are present:

$$Al + Fe + Ti = 2 + 1.42x \quad (3)$$

$$Al_{VI} + Fe_{VI} + Ti_{VI} = 2 \quad (4)$$

$$Al_{IV} + Fe_{IV} + Ti_{IV} = 1.42x \quad (5)$$

$$Al_{IV} + Al_{VI} = Al = 2 - 2x \quad (6)$$

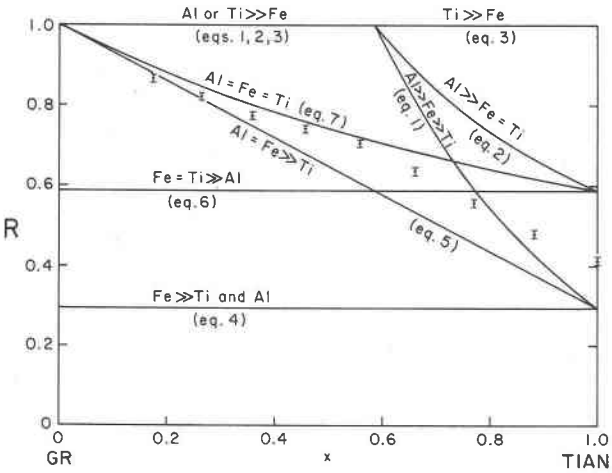

Fig. 4. Plot of the ferric distribution parameter, R, as a function of the compositional parameter, x, for samples along the GR–TIAN join synthesized at 1050° or 800°C. Curves corresponding to the ordering schemes listed in Table 4 are also shown.

$$Fe_{IV} + Fe_{VI} = Fe = 2x \quad (7)$$

$$Ti_{IV} + Ti_{VI} = Ti = 1.42x \quad (8)$$

Hence, only two site occupancies (for different elements) need be measured for complete knowledge of all the site occupancies. The Mössbauer data provide site occupancies for only one element. The lack of knowledge concerning one more site occupancy can be translated into a relationship between K_1 and K_2, the distribution coefficients for Al–Fe and Ti–Fe exchange, respectively. The latter is defined in equation (2) above; the former is defined as follows:

$$K_1 = [Al_{IV}][Fe_{VI}]/[Al_{VI}][Fe_{IV}] \quad (9)$$

By manipulation of eqs. (2) and (6–9), the octahedral occupancies may be expressed in terms of K_1, K_2, x, and R_{Fe}, as follows:

$$Al_{VI} = (2 - 2x)/(1 + K_1R_{Fe}) \quad (10)$$

$$Ti_{VI} = 1.42x/(1 + K_2R_{Fe}) \quad (11)$$

$$Fe_{VI} = 2x/(1 + R_{Fe}) \quad (12)$$

where R_{Fe} is the ratio Fe_{IV}/Fe_{VI}. By substituting these values in equation (4), an expression relating K_1 and K_2 is obtained:

$$(2 - 2x)/(1 + K_1R_{Fe}) + 1.42x/(1 + K_2R_{Fe}) + 2x/(1 + R_{Fe}) = 2 \quad (13)$$

Thus, at a given value of x, a measured value of R_{Fe} defines a relationship between K_1 and K_2. If mixing of cations at the distinct crystallographic positions conforms to an ideal cation-exchange model, the values of K_1 and K_2 should be constant at any given temperature; therefore, curves relating K_1 and K_2 for each value of x should intersect at a unique point reflecting the most appropriate values of K_1 and K_2 at that temperature. When the measured R_{Fe} values are substituted into equation (13), the curves shown in Figure 5 result, and the assumption of ideal cation-exchange behavior appears to be satisfied, because a unique point is in fact obtained for each temperature. Not only do the data seem to provide a test of the ideality of cation exchange between the sites in the solid-solution series, but the most appropriate values of K_1 and K_2 (Table 5) at the two temperatures and hence *complete* site occupancy data can also be determined. The ferric data and the calculated curves defined by values of K_1 and K_2 are compared in Figure 6.

Although the test for ideal cation exchange (Fig. 5) and the fit of the data to the distribution curves (Fig. 6) were satisfactory, there are a number of factors

suggesting that this result might be misleading. First, the ferric distribution data for the two joins lie on almost the same trends (compare Figs. 3 and 4). Secondly, the cation distribution in the AN–TIAN join does not conform to an ideal cation-exchange model, and the values of K_2 are not compatible with those for the GR–TIAN join (compare Tables 2 and 5). Thirdly, the site preferences in the GR–TIAN join become reversed between the two temperatures (Table 5). Because of these factors, additional heating experiments were made in order to evaluate the effect of temperature on the site distribution and to obtain some understanding of the kinetics of the exchange reaction.

The data and curves in Figure 6 suggested an initial test of the distribution model because, as indicated in this figure, there should be a large difference in R between samples synthesized at 800°C and those synthesized at 1050°C at the titanium-rich end of the GR–TIAN join. Subsequently, crystallization experiments at 800°C were carried out at this end of the join; the Mössbauer data for these samples are summarized in Table 6a. The ferric distribution data are almost identical with those for samples of the same composition but synthesized at 1050°C. The near coincidence of the data for the samples crystallized at the two different temperatures strongly suggests that at these temperatures the observed distribution does not approach equilibrium and that factors other than temperature alone are controlling the distribution. Further discussion of this result is presented later in the paper.

Experiments with high-temperature runs

Only at temperatures of 1200°C and above is the iron distribution observed to change significantly. Figure 7 illustrates the subtle changes induced by heating at 1220°C for 40 days a sample originally crystallized at 1050°C. The Mössbauer data for samples synthesized or heated for periods up to 6 weeks at temperatures in excess of 1200°C are listed in Table 6b and 6c for the AN–TIAN and GR–TIAN joins, respectively.

The K_2 values for the AN–TIAN join at ~1250°C appear to fit a single ideal isotherm curve, defined by a K_2 value of about 0.30 (Fig. 8). The data scatter somewhat about this curve, and this scatter may indicate that equilibrium has still not been completely attained. The ferric distribution at ~1250°C clearly conforms more closely to an ideal distribution than that at 1050°C. For the three samples on the GR–TIAN join, which are stable at 1225°C, a thermodynamic analysis based on an ideal cation-exchange model was carried out; this analysis was similar to that for the samples synthesized at 1050° and 800°C. The K_1 *vs.* K_2 plot (Fig. 9) gave a well-defined point of intersection, which defined values of 1.35 ± 0.25 for K_1 and 0.25 ± 0.05 for K_2. At this temperature (~1225°C), the values for K_2 for the different joins are compatible, unlike the situation at 1050°C.

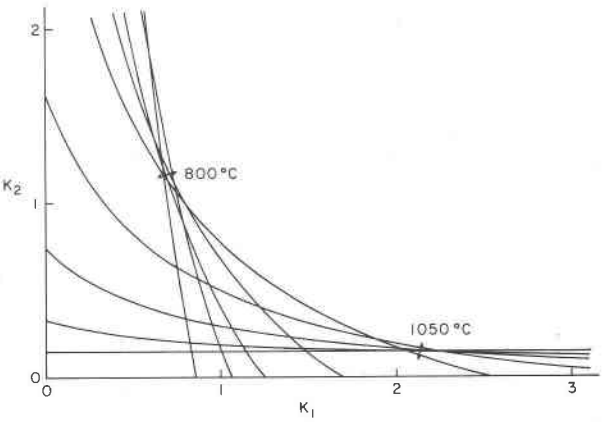

Fig. 5. Plot of the relationship between the two distribution coefficients, K_1 and K_2, defined by the Mössbauer ratio, R_{Fe}, for garnets along the GR–TIAN join. The points of intersection at the different temperatures define the most appropriate values of K_1 and K_2 for the samples.

These results suggest that at temperatures above 1200°C the cations between the different sites in the garnet structure are approaching a distribution that conforms to an ideal cation-exchange model. At such high temperatures, the equilibrium preferences of the three cations for the tetrahedral sites in the garnet structure, as defined by the values of K_1 and K_2, are in the order Al ≥ Fe > Ti. From the values of K_1 and K_2 at ~1250°C, using the relationship

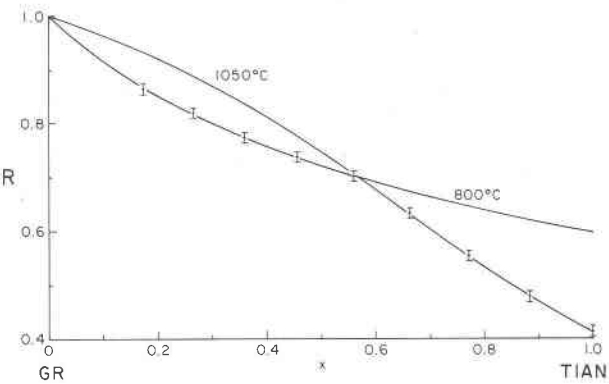

Fig. 6. Comparison of the ferric distribution parameter, R, and calculated isotherms defined by the values of K_1 and K_2 listed in Table 5 for the GR–TIAN join.

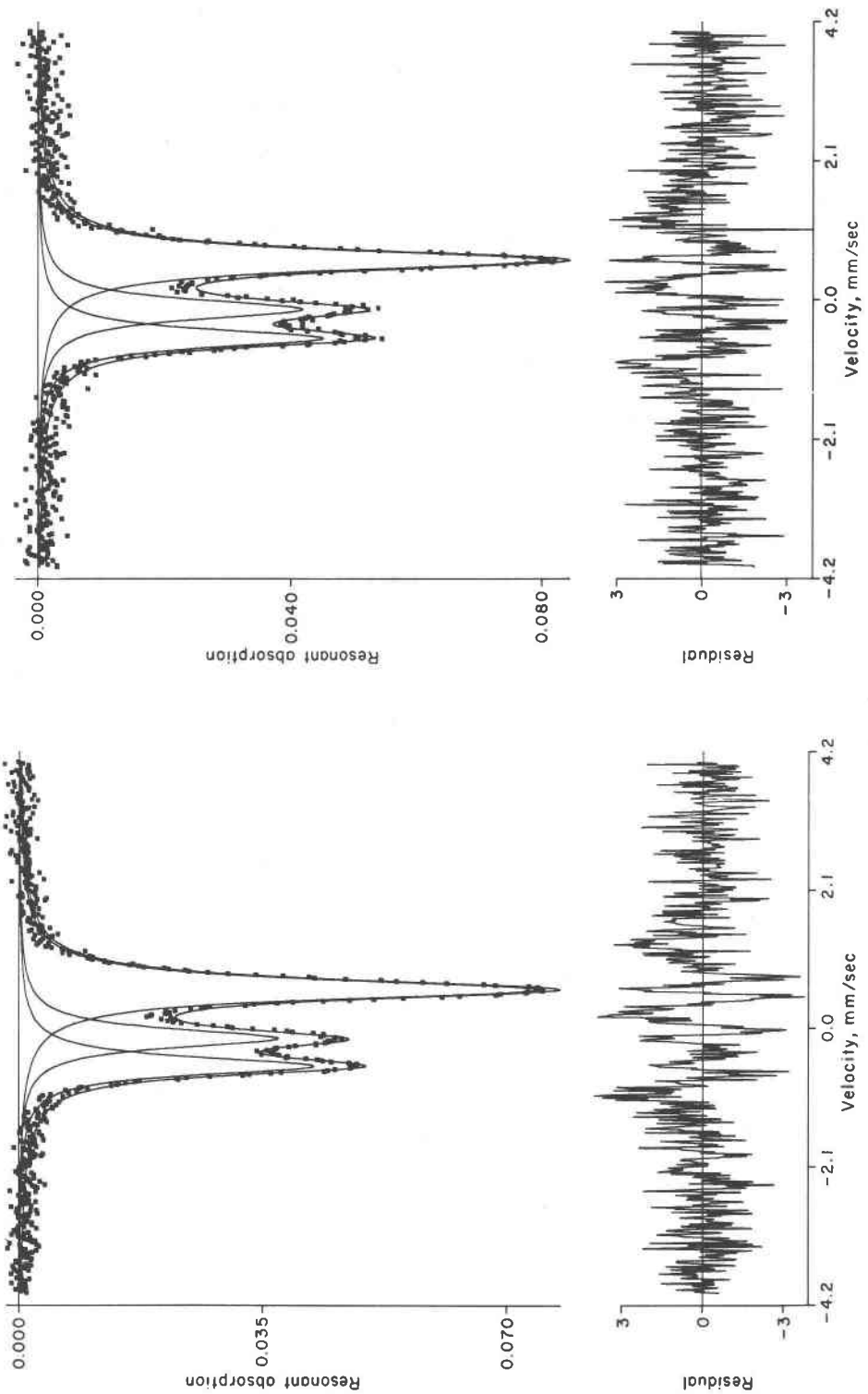

Fig. 7. Mössbauer spectra of a sample ($x = 0.883$) along the GR–TIAN join. Spectra show the small changes in distribution encountered by heating the garnet, which was initially crystallized at 1050°C (left), for 40 days at 1230°C (right).

$$\Delta G_E = RT \ln K_i$$

(where ΔG_E is the free energy of exchange, T is the temperature in °K, and R is the gas constant), a ΔG_E value of ~1 kcal/mole can be estimated for Al–Fe exchange and ~4 kcal/mole for Fe–Ti exchange. These values are similar to those estimated for other cation-exchange phenomena found in oxides and silicates (*e.g.* Virgo and Hafner, 1969; Seifert and Virgo, 1975).

Discussion

Kinetics of the order-disorder phenomena and geothermometry implications

One of the reasons for investigating the site preferences of titanium-containing garnets was to assess their potential as geothermometers and indicators of thermal histories of rocks containing such garnets. This study shows that samples synthesized or heated at temperatures above 1200°C for up to 6 weeks have an internal cation distribution that *approaches* that predicted from an ideal cation-exchange model compatible with data from both joins. Thus, it is estimated that at such temperatures a period of at least 1 or 2 months is probably required for an equilibrated state to be reached. The time needed to reach equilibrium at temperatures of 1050°C or below, therefore, may be on a time scale of years. This inference is supported by the similarity of the cation distributions in samples synthesized at 800° and 1050°C, despite synthesis times of up to 4 months for certain samples.

In addition, the maximum possible change in the ratio R (Eq. 1) is not very large except at the titanium-rich ends of the joins. Based on the order of preference for the tetrahedral site, Al ≥ Fe > Ti, determined at high temperatures, the range of values of R that can be expected for the AN–TIAN join is defined by the curves where $K_2 \approx 0.3$ and $K_2 \approx 0$ (Fig. 8). For the GR–TIAN join, values of K_1 and K_2 can be expected to be limited to >1 and <1, respectively. Hence, the area in which data for this join should plot is bounded by the curves denoted by Al >> Fe = Ti and Al = Fe >> Ti in Figure 4. This range is probably much greater than that found in practice, however, because it is unrealistic to expect complete ordering for one pair of elements while the second pair of elements shows complete disordering. Furthermore, it can be anticipated that the different values of the distribution coefficient as a function of temperature are probably mostly associated with Al and Ti, rather than Fe. This fact is a direct result of the intermediate position of ferric iron in the order of site preference. Changes in the ferric distribution as a result of a stronger preference of Ti for the octahedral sites at lower temperatures are compensated by opposite changes as a result of a stronger preference of Al for the tetrahedral site.

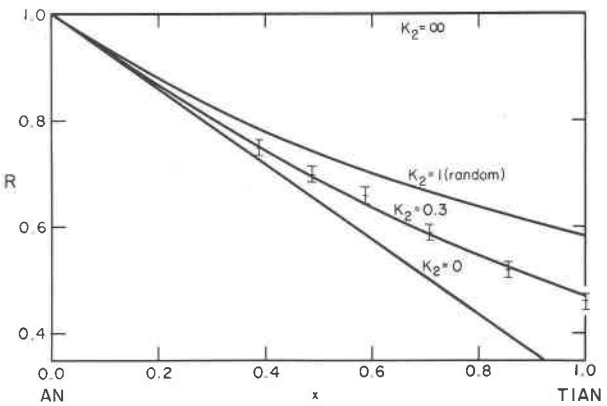

Fig. 8. Plot of the ferric distribution parameter, R, as a function of the compositional parameter, x, for samples along the AN–TIAN join synthesized at temperatures above 1200°C. Curves corresponding to different values of the distribution coefficient, K_2, are also shown.

The unfavorable kinetics, at least for these restricted compositions, and the small range of values expected for changes in the ferric distribution would appear to preclude the calibration of a useful geothermometer based on Mössbauer measurements of the ferric distribution in titanian garnets. However, the very slow kinetics for the order-disorder phenomenon may be used to indicate the crystallization process, because at low temperatures the distribution generated upon formation may be effectively "frozen-in." This aspect is discussed in detail in the next section.

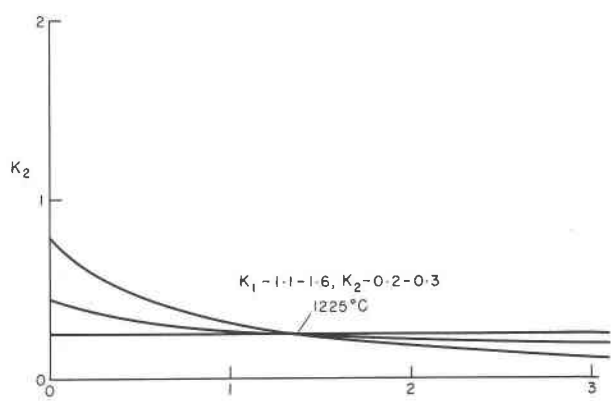

Fig. 9. Plot of the relationship between the two distribution coefficients, K_1 and K_2, defined by the Mössbauer data for garnets along the GR–TIAN join stable above 1200°C.

The extremely sluggish rate of cation exchange in the synthetic garnets is similar to that in the feldspars, because in both minerals the order-disorder exchange reactions involve both trivalent and quadrivalent cations in tetrahedral sites. The activation energy for cation exchange must reflect the strength of the bonds being broken. As bond strength depends on ionic charge, among other factors, and inversely on the coordination number, the activation energy for Al–Fe–Ti exchange in garnets and Al–Si exchange in feldspars can be expected to be two to three times greater than that for Fe^{2+}–Mg exchange between octahedral sites in chain silicates. Hence, on the basis of the standard Arrhenius equation describing rate constants, temperatures would have to be two or three times greater for Al–Fe–Ti exchange in garnets to occur at the same rate as Fe^{2+}–Mg exchange in chain silicates. Such a difference is indeed found when the "cut-off" temperatures for the two exchange processes are compared. The cut-off temperatures are those at which cation exchange is too slow to be conveniently measured in the laboratory, ~500–700K for Fe^{2+}–Mg exchange in chain silicates (Virgo and Hafner, 1969; Seifert and Virgo, 1975) and ~1500K for Al–Fe–Ti exchange in garnets.

Influence of crystallization path on the cation distribution at low temperatures

Despite the excellent fit of the data to ideal cation-exchange models (Figs. 4 and 5), the cation distributions in the GR–TIAN join, as well as in the AN–TIAN join, do not appear to have reached equilibrium when crystallized at temperatures of 1050°C and below. Indeed, because of the sluggish kinetics, it is likely that the observed cation distributions are effectively initial distributions, which were generated at the beginning of crystallization and do not change significantly during the remaining time of crystallization. Such distributions may be regarded as frozen-in.

The distinct breaks in the trends of the ferric distribution against composition (Figs. 3 and 4) indicate that more than one crystallization mechanism is needed to account for the observed initial distributions. The closely similar trends of the two joins, however, suggest that these initial distributions, and hence the crystallization mechanism, are determined primarily by the titanium content. There appear to be at least two possible mechanisms that could give rise to an initial distribution dependent only on titanium content: (1) crystallization directly from the glass, and (2) crystallization from the glass *via* metastable phases. For the first mechanism to be operative, the glass "structure" and garnet structure should be quite similar, so that the cation distribution in the glass can be retained upon crystallization. Both Mössbauer and vibrational (infrared) studies show, however, that the glass and garnet are structurally different. Mössbauer spectra of the glasses (Fig. 10) uniformly show a broad absorption doublet, which has parameters intermediate to those of octahedral and tetrahedral ferric iron in a titanian garnet. Such spectra were found to be identical regardless of whether the composition was that of AN or TIAN, or from along the GR–TIAN join. These results suggest that the garnet and glass structures are not directly related. Similarly, vibrational spectra of the garnets and glasses indicate the lack of an obvious structural relationship. As can be seen in Figure 11, the main Si–O stretching vibrations in the garnets compared with those of the respective glasses are at significantly lower frequencies. This observation suggests that there may be Si–O–Si linkages in the glass, because it is well known that Si–O polymerization effectively increases the frequency of vibration. Less direct evidence that the garnets and their glass are structurally quite different is the fact that in neither join does a garnet crystallize directly from the glass (Huckenholz, 1969; Hölzl, 1975). Instead, depending on composition, the subliquidus phases for these garnet compositions are gehlenite, pseudowollastonite, or perovskite. Hence, significant structural rearrangement and movement of ions are necessary if the garnets are to crystallize directly from the glasses, and any relative ordering of the Al, Fe, and Ti cations between the octahedral and tetrahedral sites in the glasses is unlikely to be retained in the corresponding garnets.

For the above reasons, the alternative hypothesis involving the formation of metastable phases in the crystallization process must be evaluated. Evidence for this process is provided by Huckenholz (1969), who reported that, for low-titanium compositions, wollastonite and hematite were found in addition to garnet in synthesis runs of short duration. On further heating, these phases diminished with time, until only garnet remained. Furthermore, glasses of high titanium content usually contained perovskite upon being quenched. Both wollastonite and perovskite occur prominently in the high-temperature breakdown reactions that separate liquid and garnet fields in the garnet phase diagrams (Huckenholz, 1969; Hölzl, 1975). Whether $CaSiO_3$ or $CaTiO_3$ is found at a given composition depends entirely on the Ti/Si ratio.

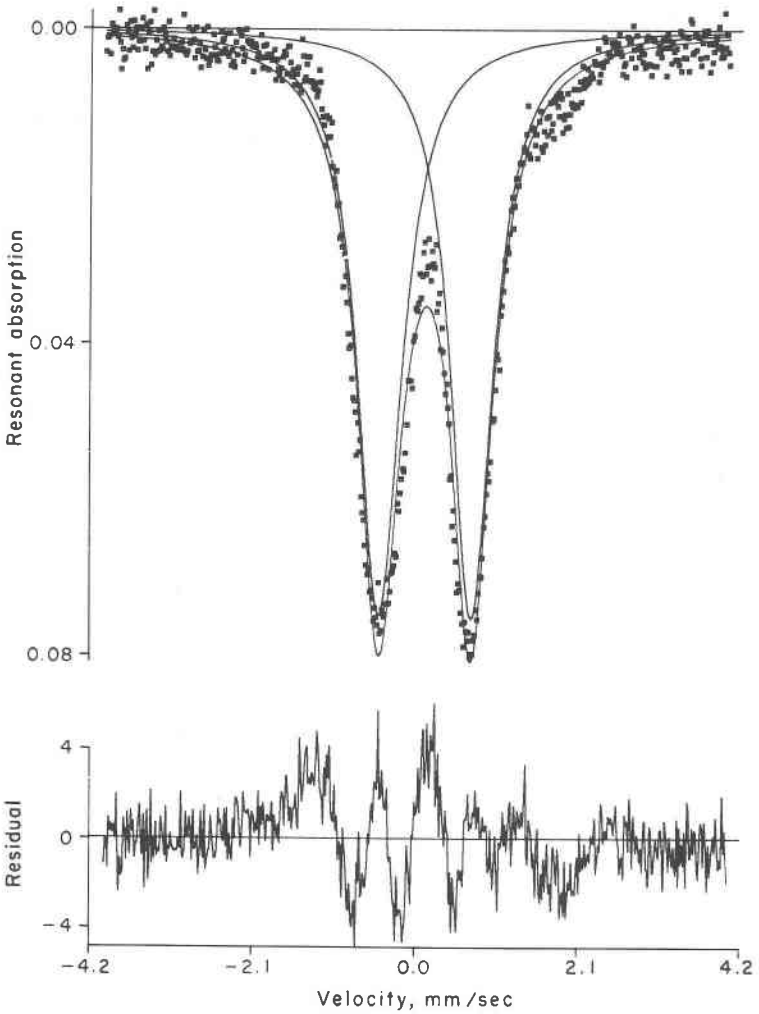

Fig. 10. Mössbauer spectrum of glass of andradite garnet composition. The spectrum is fitted to only a single doublet (IS = 0.31, QS = 1.19; *cf.* titanium garnets, Virgo and Huckenholz, 1974; Huggins *et al.*, 1975).

Hence, it is postulated that the initial, frozen-in cation distributions in the garnet and the break in the distribution trends are determined by the following crystallization paths (Fig. 12):

Si-rich compositions: glass →
$(CaSiO_3$ + glass + garnet) → garnet

Ti-rich compositions: glass →
$(CaTiO_3$ + glass + garnet) → garnet

The reaction between the metastable $CaSiO_3$ or $CaTiO_3$ and glass would then give rise to the observed distribution of cations in the garnet. We suggest that these metastable phases act as nucleation sites for the formation of the garnet; because $CaSiO_3$ does not fix Al, Fe, or Ti in a given coordination site, the distribution of these cations in the Ti-poor garnets is close to random. Conversely, because $CaTiO_3$ does contain Ti in octahedral coordination, Ti-rich garnets formed via metastable $CaTiO_3$ may contain a disproportionately large amount of octahedrally coordinated Ti in the initial distribution.

In view of the influence of the crystallization path on the initial cation distribution in garnets discussed above, it is instructive to compare the cation distribution in garnets formed in other ways with the well-defined trend for the ratio R as a function of titanium content established in this study. The result obtained by Burns (1972) for the composition $Ca_3Fe_2TiSi_2O_{12}$, which indicates that no titanium is present on the tetrahedral sites, differs significantly from the trend for garnets crystallized from glasses, and may reflect

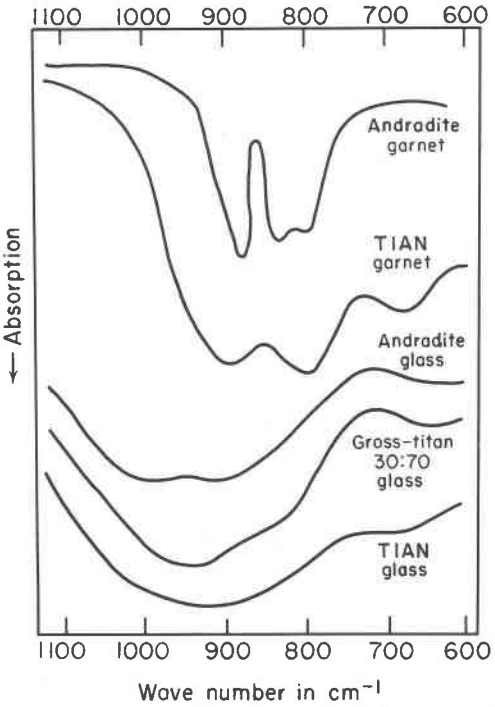

Fig. 11. Comparison of vibrational spectra of garnets and glasses showing Si–O stretching bands at higher frequencies for glasses.

a completely different trend for samples synthesized by sintering coprecipitated gels at 1050°C for 20 hours (Ito and Frondel, 1967). Similarly, natural garnets from serpentinized peridotites (Burns and Burns, 1971; Huggins *et al.*, 1977) appear to lack ferric iron in tetrahedral coordination in the Mössbauer spectrum, and may lie on yet another initial ferric distribution trend.

Crystal-chemical considerations

The order of tetrahedral site preferences inferred for synthetic titanium silicate garnets, Al ≥ Fe > Ti, may be compared with the site preferences found in other synthetic garnets. A number of studies using different techniques have shown that aluminum favors the tetrahedral site relative to iron in $Y_3Fe_{5-x}Al_xO_{12}$ (e.g., Geller *et al.*, 1964; Borghese, 1967; Czerlinsky and Macmillan, 1970.) In this garnet solid-solution series, the data do not conform to an ideal solid solution model (Fischer *et al.*, 1975), and there appears to be some disagreement between results obtained with different techniques. The relative site preferences of iron and titanium have been studied in $Y_{3-x}Ca_xTi_xFe_{5-x}O_{12}$ (Espinosa, 1964; Geller *et al.*, 1965) and in $Ca_3Fe_{2-x}Ti_{2x}V_{3-x}O_{12}$ (Nakayama *et al.*, 1971). In both series of garnets, titanium was found to favor strongly the octahedral site relative to ferric iron; in neither study, however, was a detailed thermodynamic analysis of the data attempted. The site preferences of other cations, which have been evaluated in synthetic garnets, include Ga (Geller *et al.*, 1966; Czerlinsky, 1969; Mueller and Ghose, 1970) and Zr^{4+}, Sn^{4+}, Sc^{3+}, Cr^{3+}, and In^{3+} (Geller, 1967). Gallium has a stronger preference than either Al or Fe for the tetrahedral site, whereas the other five cations are found exclusively in octahedral sites. Hence the experimentally determined preferences for the tetrahedral sites in garnets are in the order Ga > Al > Fe > Ti >> Sc, In, Zr, Sn, Cr. Of these nine cations only Cr^{3+} has an octahedral site preference arising from crystal-field effects, so that in attempting to rationalize the order for the remaining eight cations, this factor need not be considered. The fact that garnets of the formulae $A_3^{2+}B_2^{3+}C_3^{4+}O_{12}$, $A_3^{2+}B_2^{3+}C_3^{4+}O_{12}$, $A_3^{2+}B_2^{4+}C^{4+}D_2^{3+}O_{12}$, and $A_2^{2+}B^{3+}C_2^{4+}D_3^{3+}O_{12}$ have all been synthesized indicates that ionic charge is not the dominant factor in determining site preferences. If ionic size were the only criterion, the predicted order of tetrahedral site preferences would be Al >> Ti > Ga > Fe >> Sn > Zr > Sc >> In, based on Shannon and Prewitt's (1969) ionic radii. This order is indeed essentially correct, because all ions listed above that are larger than Fe^{3+} are found exclusively in octahedral coordination; however, the inferred order for those cations found in both octahedral and tetrahedral coordination, Ga (0.62) > Al (0.53) > Fe (0.645) > Ti (0.605), is not compatible with ionic size. Dowty (1971) proposed that electronegativity might be an additional factor that determines cation site preferences in titanium silicate garnets. We therefore suggest that the experimentally established order of tetrahedral site prefer-

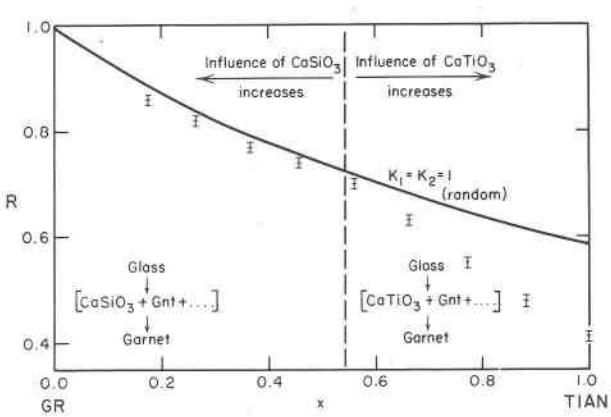

Fig. 12. Crystallization paths suggested for the GR–TIAN join to account for initial cation distribution in the garnet.

ence reflects electronegativity as well as ionic size. With this factor the following order may be predicted, Fe (1.9) > Ga (1.7) > Al, Ti (1.6), based on Batsanov's (1968) electronegativity scale; hence it is quite conceivable that the influence of both factors would explain the observed order of site preferences. The use of electronegativity as a factor determining site preference suggests that cations with a larger electronegativity favor the tetrahedral site over the octahedral site in the garnet structure.

Conclusions

In this study, the relative preferences of Al, Fe, and Ti for the tetrahedral sites in garnets have been demonstrated to be in the order Al ≥ Fe > Ti and confirm the predictions made by Hartman (1969). This result can be rationalized if both ionic size and electronegativity are considered as important factors controlling the site preferences. The kinetics for exchange appear to be very slow; garnets formed from glasses at temperatures less than 1050°C appear to have their initial cation distribution frozen-in despite heating times of up to 4 months. Indeed, it appears that the distribution of ferric iron in the garnet structure is probably determined mainly by the formation reaction, unless sufficiently long heating times and high temperatures have been used, when equilibrium may have been approached.

Acknowledgments

The authors are grateful to E. Hölzl (University of Munich) for supplying the synthetic garnets on the GR–TIAN join. The authors also acknowledge discussions and reviews of preliminary and final versions of this manuscript by R. H. McCallister, L. W. Finger, H. S. Yoder, Jr., B. J. Wood, and S. S. Hafner.

The last-named author (H.G.H.) gratefully acknowledges the support given him by the Deutsche Forschungsgemeinschaft to carry out parts of this study.

References

Batsanov, S. S. (1968) The concept of electronegativity. Conclusions and prospects. *Russ. Chem. Rev., 37,* 332–351.

Borghese, C. (1967) Cation distributions in multisublattice ionic crystals and applications to solid solutions of ferrimagnetic garnets and spinels. *J. Phys. Chem. Solids, 28,* 2225–2237.

Burns, R. G. (1972) Mixed valencies and site occupancies of iron in silicate minerals from Mössbauer spectroscopy. *Can. J. Spectrosc., 17,* 51–59.

——— and V. M. Burns (1971) Study of the crystal chemistry of titaniferous garnets by Mössbauer spectroscopy (abstr.). *Geol. Soc. Am. Abstr. Progr., 3,* 519–520.

Czerlinsky, E. R. (1969) Cation distributions in gallium-substituted yttrium iron garnets by Mössbauer effect spectroscopy. *Phys. Status Solidi, 34,* 483–493.

——— and R. A. Macmillan (1970) Cation distributions in aluminum-substituted yttrium iron garnets by Mössbauer effect spectroscopy. *Phys. Status Solidi, 41,* 333–342.

Dollase, W. A. (1975) Statistical limitations of Mössbauer spectral fitting. *Am. Mineral., 60,* 257–264.

Dowty, E. (1971) Crystal chemistry of titanian and zirconian garnet: I. Review and spectral studies., *Am. Mineral., 56,* 1983–2009.

——— and R. Mark (1968) Titanian garnets: Mössbauer and infrared spectroscopy (abstr.). *Geol. Soc. Am. Spec. Pap., 121,* 80.

Espinosa, G. P. (1964) A crystal chemical study of titanium (IV) and chromium (III) substituted yttrium iron and gallium garnets. *Inorg. Chem., 3,* 848–850.

Fischer, P., W. Mälg, P. Roggwiller and E. R. Czerlinsky (1975) Cation distributions of Y–Fe–Al garnets. *Solid State Commun., 16,* 987–992.

Geller, S. (1967) Crystal chemistry of the garnets. *Z. Kristallogr., 125,* 1–47.

———, J. A. Cape, G. P. Espinosa and D. H. Leslie (1966) Gallium substituted yttrium iron garnet. *Phys. Rev., 148,* 522–524.

———, R. C. Sherwood, G. P. Espinosa and H. J. Williams (1965) Substitution of Ti^{4+}, Cr^{3+} and Ru^{4+} ions in yttrium iron garnet. *J. Appl. Phys., 36,* 321.

———, H. J. Williams, G. P. Espinosa and R. C. Sherwood (1964) Importance of intrasublattice magnetic interactions and of substitutional ion type in the behaviour of substituted yttrium iron garnets. *Bell Syst. Tech. J., 43,* 565–623.

Hartman, P. (1969) Can Ti^{4+} replace Si^{4+} in silicates? *Mineral. Mag., 37,* 366–369.

Hölzl, E. (1975) *Synthese und Stabilität von Titangranditmischkristallen im System CaO–Al_2O_3–Fe_2O_3–SiO_3–TiO_2.* Inaugural dissertation, University of Munich.

Howie, R. A. and A. R. Woolley (1968) The role of titanium and the effect of TiO_2 on the cell size, refractive index and specific gravity in the andradite–melanite–schorlomite series. *Mineral. Mag., 36,* 775–790.

Huckenholz, H. G. (1969) Synthesis and stability of Ti–andradite. *Am. J. Sci., 267A,* 209–232.

Huggins, F. E., D. Virgo, E. Hölzl and H. G. Huckenholz (1975) Distribution of Al, Fe^{3+} and Ti^{4+} between the octahedral and tetrahedral sites in garnets between $Ca_3Al_2Si_3O_{12}$ and $Ca_3Fe_2Ti_{1.416}Si_{1.584}O_{12}$. *Carnegie Inst. Wash. Year Book, 74,* 579–585.

———, ——— and H. A. Huckenholz (1977) Titanium-containing silicate garnets. II. The crystal chemistry of melanites and schorlomites. *Am. Mineral., 62,* in press.

Isaacs, T. (1968) Titanium substitutions in andradites. *Chem. Geol., 3,* 219–222.

Ito, J. and C. Frondel (1967) Synthetic zirconium and titanium garnets. *Am. Mineral., 52,* 773–781.

Kunitz, W. (1936) Die Rolle des Titans und Zirkoniums in den gesteinsbildenden Silikaten. *Neues Jahrb. Mineral. Geol., Beil. Band, 70A,* 385–466.

Lehijärvi, M. (1967) Titaanipitoisten Andratiitigranaattien Vyöhykkeisyydestä. *Geologi, 18,* 102–103.

Moore, R. K. and W. B. White (1971) Intervalence electron transfer effects in the spectra of the melanite garnets. *Am. Mineral., 56,* 826–840.

Mueller, R. F. and S. Ghose (1970) Thermodynamic behavior of Ga^{3+}, Al^{3+} and Fe^{3+} distributions in garnets. *Am. Mineral., 55,* 1932–1944.

Nakayama, Y., T. Yamadaya and M. Asanuma (1971) Magnetic properties of titanium substituted calcium–vanadium garnets. In Y. Hoshino, S. Iida and M. Sugimoto, Eds., *Ferrites: Pro-*

ceedings of an International Conference, p. 533–535. University Park Press, Baltimore.

Navrotsky, A. (1975) Thermodynamics of formation of some compounds with the pseudobrookite structure and of the $FeTi_2O_5$–Ti_3O_5 solid solution series. *Am. Mineral., 60,* 249–256.

Ruby, S. (1973) Why MISFIT when you already have χ^2? In I. J. Gruverman and C. W. Seidel, Eds., *Mössbauer Effect Methodology,* vol. 8, p. 263–276. Plenum Press, New York.

Seifert, F. A. and D. Virgo (1975) Kinetics of the Fe^{2+}–Mg, order-disorder reaction in anthophyllites: Quantitative cooling rates. *Science, 188,* 1107–1109.

Shannon, R. D. and C. T. Prewitt (1969) Effective ionic radii in oxides and fluorides. *Acta Crystallogr., B25,* 925–946.

Tarte, P. (1959) Recherches sur le spectre infrarouge des silicates: II. Détermination du rôle structural du titane dans certains silicates. *Silicates Industriels, 25,* 171–175.

——— (1965) Étude expérimental et interprétation du spectre infra-rouge des silicates et des germanates. Application à des problèmes structuraux relatifs à l'état solide. *Acad. R. Belg. Classe Sci. Mem., 35,* No. 4a, 260 p.; No. 4b, 134 p.

Virgo, D. and S. S. Hafner (1969) Fe^{2+},Mg order-disorder in heated orthopyroxenes. *Mineral. Soc. Am. Spec. Pap., 2,* 67–81.

——— and H. G. Huckenholz (1974) Physical properties of synthetic titanium-bearing grandite garnets. *Carnegie Inst. Wash. Year Book, 73,* 426–433.

Weber, H. P., D. Virgo and F. E. Huggins (1975) A neutron-diffraction and ^{57}Fe Mössbauer study of a synthetic Ti-rich garnet. *Carnegie Inst. Wash. Year Book, 74,* 575–579.

Manuscript received, June 28, 1976; accepted for publication, November 18, 1976.